VOL. 12, NO. 12, DECEMBER 1975 J. SPACECRAFT

Aeroballistics of a Terminally Corrected Spinning Projectile (TCSP)

Frank J. Regan*
Naval Surface Weapons Center, White Oak Laboratory, Silver Spring, Md.

and

Jack Smith†
Sanders Associates, Nashua, N. H.

This paper discusses the aerodynamic aspects and ballistic advantages of a method for providing terminal guidance to the Mk 41 projectile. Guidance and control functions are contained in a single unit, which is adaptable to the Mk 41 fuze-well. This unit contains all the required power system, sensors, and aerodynamic controls. These controls consist of a set of four canards in a cruciform arrangement. An overview is presented of the system concept. Indications are given of the increased effectiveness of the guided projectile over the conventional unguided round.

Nomenclature

C_m = pitching moment coefficient, M_y/QSd
C_{m_α} = pitching moment derivative, $\partial C_m/\partial\alpha$
C_{m_q} = damping-in-pitch derivative, $\partial C_m/\partial\hat{q}$
C_N = normal force coefficient, $-F_z/QS$
C_{N_α} = normal force derivative, $\partial C_N/\partial\alpha$
$C_{N_{p\alpha}}$ = Magnus force derivative, $\partial^2 C_N/\partial\hat{p}\partial\alpha$
$C^c_{N_\delta}$ = fin effectiveness derivative, $\partial C^c_N/\partial\delta$
C_n = yawing moment coefficient, M_z/QSd
$C_{n_{p_\alpha}}$ = Magnus moment derivative, $\partial^2 C_n/\partial\hat{p}\partial\alpha$
C_y = side force coefficient, F_y/QS
d = reference length, body diameter
F_x, F_y, F_z = forces along X, Y, Z axes
I_a = axial moment of inertia
I_T = transverse moment of inertia
K_a = axial radius of gyration, $(I_a/md^2)^{1/2}$
K_T = transverse radius of gyration, $(I_T/md^2)^{1/2}$
M_x, M_y, M_z = moment about X, Y, Z axes
m = mass
n = maneuvering load factor
p = spin rate
$\hat{p}$ = reduced spin rate, $pd/2V$
Q = dynamic pressure
q = pitch rate
$\hat{q}$ = reduced pitch rate, $qd/2V$
S = reference area
W = weight
X = center-of-pressure position
α = angle of attack
β = angle of sideslip
ρ = atmospheric density
ξ = complex angle of attack
δ = fin-cant angle

Superscripts

B = body
c = canard
T = total

Subscripts

a = axial
B = body
c = canard
M = Magnus
ss = steady-state or trim conditions
T = transverse

Presented as Paper 74-796 at the AIAA Mechanics and Control of Flight Conference, Anaheim, Calif., August 5-9, 1974; submitted August 21, 1974; revision recieved May 9, 1975.

Index categories; LV/M Dynamics and Control; LV/M System and Component Ground Testing; LV/M Guidance Systems (including Command and Information Systems).

*Experimental Aerodynamics Division. Member AIAA.
† Director of Projectile Guidance. Member AIAA.

Introduction

IN long-range bombardment, uncertainties in geodetics, atmospheric properties, and winds, coupled with variation in projectile mass and mass distribution, gun wear, and chamber pressure distribution, all result in an uncertainty in projectile impact location. Weapon effectiveness depends on a sequential set of corrective commands from, say, a spotter. An empirical method such as this might be acceptable against a stationary target of limited defensive capability. However, against a maneuverable, high-speed offensive weapon a gun system must function within a response time of a few seconds. A corrective algorithm based on the performance of earlier rounds is obviously inadequate. Rather, what is required is the existence of a guidance and control capability that is an integral part of each projectile.

A particular example of an operational situation in which projectile guidance is essential is in shipboard defense against the cruise missile. The essence of such an encounter is illustrated in Fig. 1. A ship whose main defensive armament against aerial targets is 5-in. deck guns is shown under attack by an antiship cruise missile. Under such demanding conditions, bias errors associated with this system severely limit the effectiveness of the defense. However, dispersion errors may be greatly reduced by adding terminal guidance late in the trajectory.

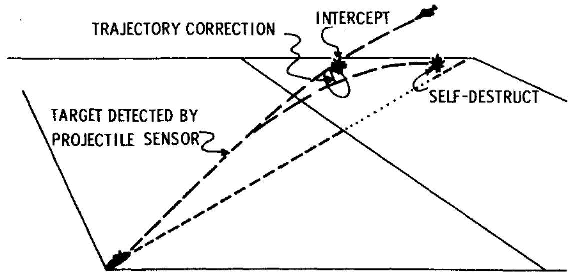

Fig. 1 System concept.

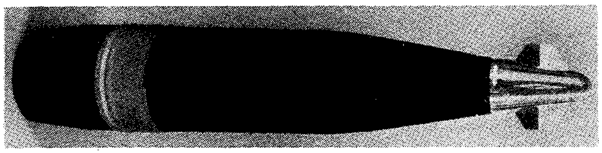

Fig. 2 Mk 41 projectile with terminal guidance.

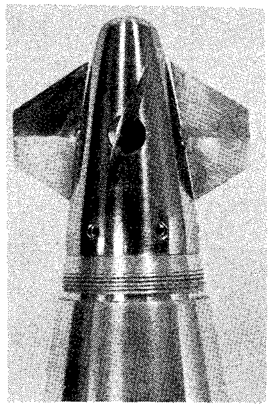

Fig. 3 Canard control frame of 2/5 scale wind tunnel model.

The decision to use terminal guidance was made after other possible improvements to the gun system effectiveness were considered. Studies were made of various system components such as guns, fire control computers, fuzes, and projectile design. The conclusion reached was that the most significant improvement that could be made in overall system effectiveness would be to provide a projectile-borne terminal guidance capability.

Guidance Package

Guidance implies the need for some means of altering the projectile trajectory to reduce miss distance. A general examination of the problem of projectile guidance might lead to a number of possibilities. For example, while the technique of jet interaction might remove the sensitivity that an aerodynamic control has to projectile speed, the complications of reservoir and conduits rule this technique out. Even a restriction to aerodynamic controls would leave open the question of control location. Base location of control fins would have certain advantages, as will be seen, in increasing gyroscopic stability. However, rear-mounted fins would be difficult to use with an existing conventional projectile. The most attractive location for control fins for the terminal guidance of an otherwise conventional projectile is certainly in the most forward part of the projectile. Such a location permits the entire guidance unit—sensors, power systems, proximity fuze, S&A booster, and aerodynamic controls—to be a self-contained package. This package can then become an integral part of the projectile through an operation no more complicated than mounting the fuze. In fact, the guidance unit becomes, in a sense, an advanced fuze, containing not only the fuze capability for warhead activation but the additional capacity to provide terminal guidance.

The Mk 41 projectile with the guidance unit in place is shown in Fig. 2. The canard fins used for controlling projectile angle of attack are conspicuous. During passage of the projectile through the gun tube, setback locks the canard frame to the projectile proper. Once the projectile emerges from the gun (and setback forces are removed), the canard frame derotates from the projectile spin rate of about 220 rps to a spin rate of 5-10 rps in an interval of about 200 msec. One pair of opposing canards can be rotated about a common axis of articulation to generate the required aerodynamic control moments; the other pair of canards is at a small fixed angle of cant (about 0.1°). The large canard area (and the large resulting roll-damping moment) causes the rapid canard frame despin; the fin cant gives the frame a residual rolling moment in a direction opposite to that of the shell. During the guidance phase this slight rotation rate is stopped relative to inertial space and in such an orientation that the axis of articulation is normal to the plane defined by the shell axis of symmetry vector and a vector from the shell center of gravity to the target. This plane is not necessarily coincident with the angle-of-attack plane and so loads normal to, as well as in, the target plane are generated. The guidance system continuously changes the orientation of the canard frame to keep most of the aerodynamic loads in the target plane.

The generated aerodynamic load results in the development of a trim angle of attack. The trim angle generates the required body lift to steer the projectile. Because of the continuous decrease in projectile velocity, g's available for maneuverability are limited. Since proportional navigation makes maximum effective use of g-capability, it was chosen as the guidance law.

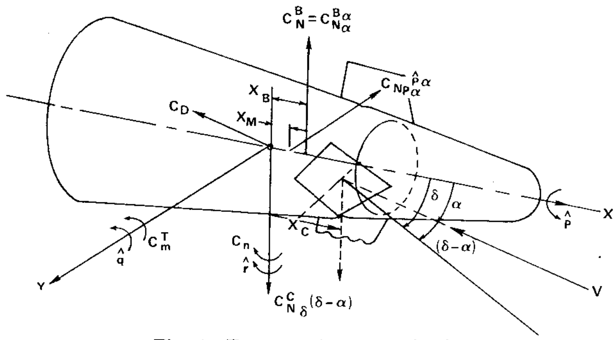

Fig. 4 Forces acting on projectile.

Aerodynamic Controls

The aerodynamic controls have been identified in Fig. 2. A clearer view of the canard frame is shown in Fig. 3. Subsequently, a discussion will be given of the various aerodynamic and packaging constraints that were imposed on the canard design. For the present it will be assumed that a trim-generating capability is available in the canards. Three questions should be addressed regarding these canards. First, can the canards be used to trim a conventional spinning shell? Second, what is the effect of the canards upon the projectile gyroscopic and dynamic stability? Third, what is the maneuverability of the projectile with the canards in place?

Projectile Trim

In considering projectile trim it is helpful to illustrate the essential forces acting on the projectile. Figure 4 is a graphical representation of the aerodynamic loads acting on the projectile. These loads may be represented in terms of the total pitching moment, C_m^T, as

$$C_m^T = X_B C^B_{N_\alpha}\alpha - X_c C^c_{N_\delta}(\delta-\alpha) + C^{Bc}_{m_q}\hat{q} + X_M C^B_{N_{p_\alpha}}\hat{p}\beta \tag{1}$$

This equation indicates that the pitching moment is comprised of four distinct constituents. These contributions are identified by the four terms on the right as: the static moment due to and proportional to the body angle of attack α; the static moment due to the canard and proportional to the canard local angle of attack $(\delta-\alpha)$; the pitch damping moment due to both body and canards and proportional to the reduced pitch-rate $\hat{q}$; the Magnus moment due to the body and proportional to the product of the body reduced spin rate $\hat{p}$ and angle of sideslip β. Since the canard frame rapidly despins upon emergence from the gun, it is assumed to make no Magnus contribution.

In order to avoid excessive clutter, Fig. 4 is presented without sideslip β indicated. Consistent with Eq. (1), sideslip is defined as the angle between the axis of symmetry X and the component of the velocity vector V in the XY plane; the definition of the angle of attack remains as the angle between the axis of symmetry X and the component of the velocity vector V in the XZ plane. Slightly different definitions of $\{\alpha,\beta\}$ might be used, but the restriction of these quantities to small values would leave Eq. (1) unchanged. Additional complications in Eq. (1) would arise if the canard axis of articulation of AA' is allowed to take an arbitrary rotation with respect to the Y axis. However, since the goal here is to point out some of the conditions at trim and not to attempt a lengthy dynamic analysis, Eq. (1) will be assumed sufficiently representative of conditions at trim.

Returning now to Eq. (1), trim will be defined as existing when $\alpha=\alpha_{ss}$, and $C^T_m=0$, $\beta=0$, $\hat{q}=0$. With these simplifications Eq. (1) may be written as

$$\alpha_{ss}/\delta = X_c C^c_{N_\delta}/[x_B C^B_{N_\delta} + x_c C^c_{N_\delta}] \tag{2}$$

Equation (2) provides the trim angle, α_{ss}, per unit fin cant, δ. Before commenting upon Eq. (2), we will give an alternate derivation. This approach will consider trim conditions using the classical ballistic equation, which includes body spin and body mass and mass distribution.

Figure 4 is a simplification of the classical ballistic load formulation. Fox example, there also exists a second complete set of moments similar to those given in Eq. (1) if the velocity vector V is not contained in the XZ plane. This second set of moments would follow from Eq. (1) by replacing m with n, α with β, and q with r. The canard would not make any contribution to the yawing moment if AA' is normal to the XZ plane as the second set of canards is at a fixed differential cant.

The formulation of the ballistic problem in terms of these moments leads to the classical ballistic equation as formulated by Murphy[1]

$$\xi'' + (H-iP)\xi' - (M+iPT)\xi = iA \tag{3}$$

where

$$M = C^{*T}_{m_\alpha} K_T^{-2} = K_T^{-2}[X_B C^{*B}_{N_\alpha} + X_c C^{*c}_{N_\delta}] \tag{4a}$$

$$T = [(C^{*T}_{N_\alpha} - C^*_D) + K_a^{-2} X_m C^{*B}_{Np_\alpha}]$$

$$\approx C^{*T}_{N_\alpha} + K_a^{-2} C^{*B}_{Np_\alpha} \approx K_a^{-2} C^{*B}_{Np_\alpha} \tag{4b}$$

$$A = -K_T^{-2} X_c \; C^{*c}_{N_\delta} \; \delta \tag{4c}$$

$$H = C^{*T}_{N_\alpha} - 2C^*_D - K_T^{-2} \; C^{*B}_{mq} c \tag{4d}$$

$$P = 2(K_a/K_T)^2 \; \hat{p} \tag{4e}$$

where the presence of an asterisk indicates an aerodynamic derivative or coefficient multiplied by the relative density $(\rho sd/2m)$. Again Eq. (4c) shows that the asymmetry is in only one set of canards, pitch, in this case, as the other set is at a fixed differential cant.

If steady-state conditions are defined to exist when

$$\xi'' = \xi' = 0\,; \quad \xi = i\alpha_{ss} + \beta_{ss} \tag{5}$$

Eq. (3) becomes

$$\xi_{ss} = -iA/(M+iPT) \tag{6a}$$

$$= -iA(M-iPT)/[M^2+P^2T^2] \tag{6b}$$

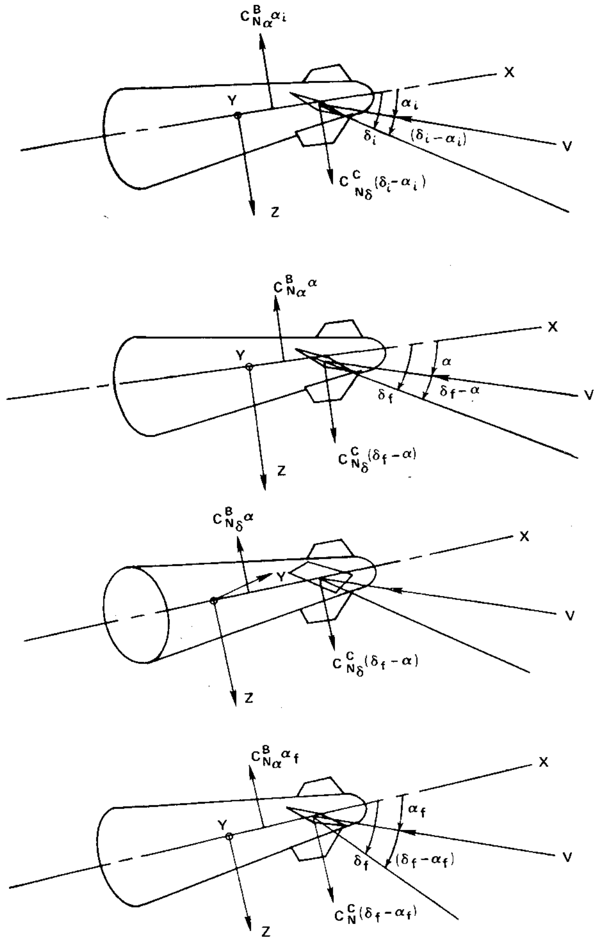

Fig. 5 Flight mechanics.

Now if the right-hand side of Eq. (6) is normalized by M^2 and expanded in a Taylor series to the second term in PT/M, the result is

$$\alpha_{ss} = -(A/M)\,[1-(PT/M)^2] \tag{7a}$$

$$\beta_{ss} = -(A/M)\,[PT/M] \tag{7b}$$

Now, using the definitions of Eq. (4), it is fairly straightforward to rewrite Eq. (7) as

$$\frac{\alpha_{ss}}{\delta} = \frac{X_c C^c_N \delta}{[X_B C^B_{N_\alpha} + X_c C^c_{N_\delta}]} \Bigg[1 - \hat{p}^2 \left\{ \frac{2C^B_{Np_\alpha}}{X_B C^B_{N\alpha} + X_c C^c_{N\delta}} \right\}^2 \Bigg] \tag{8a}$$

$$\frac{\beta_{ss}}{\delta} = \hat{p} \left\{ \frac{2X_c C^c_{N\delta} C^B_{Np_\alpha}}{(X_B C^B_{N\alpha} + X_c C^c_{N\delta})^2} \right\} \tag{8b}$$

In the previous expressions the asterisk has been omitted since the aerodynamic coefficients appear only in ratios.

In examining Eq. (8) one may reach two interesting conclusions. Equation (8a) shows that spin can alter the pitch angle in trim α_{ss} only as a second-order effect. Equation (8b) indicates that a pitch asymmetry δ, in the presence of spin, causes a sideslip angle of trim, β_{ss}. However, Eq. (8) may be simplified when it is recognized that $\hat{p}$ is 0 (10^{-1}) and the terms in braces, in both equations, are 0(1). Thus Eq. (8a) may be written as

$$\alpha_{ss}/\delta = X_c C^c_{N_\delta}/\,(X_B C_{N\delta}^B + X_c C_{N\delta}^c) \tag{9}$$

with the trim angle in sideslip β_{ss} no larger than a tenth of α_{ss} and is, for present purposes, negligible. It will now be noted that Eqs. (2) and (9) are identical. Thus the presence of body spin, as encountered in any practical projectile, has a negligible effect on the trim angle of attack per unit fin cant.

One interesting comment may now be made with regard to trim. In Fig. 4 it will be noted that angle of attack is defined positive with the body vertex above the velocity vector, and canard angle is defined positive with canard leading edge downward. Equation (9) shows that the statically unstable projectile trims body vertex upward for canard leading edge downward—exactly the reverse of a statically stable, nonspinning, conventional, canard-controlled missile.

In developing Eq. (8) the assumption was made that the projectile with canards in place is inherently stable—the canards serve only to vary the trim angle. By letting $\xi'' = \xi' = 0$, the damped transients are ignored. At this point stability must be accepted as a premise subject to later substantiation by either a numerical integration of the equations of motion or by some kind of data coverage of a projectile firing. Trim stability and performance characteristics of the projectile were investigated using a six-degree-of-freedom simulation of the configuration. In the simulation, with the shell subjected to open-loop canard deflections, steady-state trim angles of attack were obtained corresponding with those measured in the wind tunnel. The projectile oscillated about these values, with a double amplitude of less than 1° and with a fairly low damping ratio. Subsequent simulations of a fully guided round showed that these small oscillations did not degrade the predicted performance. Unguided firings have substantiated these conclusions to some extent. These firings have shown that there is only a 2% range degradation with canards in place, indicating freedom from a large-amplitude limit cycle.

Rather than present the results of these six-degree-of-freedom simulations, a brief description of projectile motion after canard deflection will probably be sufficient. A pictorial representation of this motion is given in Fig. 5. Assuming that a positive angle of trim is desired, the canard leading edge must be deflected downward. The first motion of the projectile will be in the direction of the torque, i.e., nose downward. Since this torque vector is orthogonal to the angular momentum vector, the projectile will precess nose left out of the angle-of-attack plane (plane of the paper). The out-of-plane motion develops an angle of sideslip β; the resulting aerodynamic moment, orthogonal to angular moment vector, precesses the nose upwards. This angular motion continues until the projectile has reached a trim angle of attack [as predicted by Eq. (9)].

Projectile Stability

Murphy[1] has shown from the solution to Eq. (2) that the projectile has two modes of motion and that the exponential damping coefficients of this motion, λ_1 and λ_2, might be expressed as

$$\lambda_{1,2} = (K_T^{-2}/2)\; C_{m_q}^{*B_c}\{1 \pm [S_d - 1]/[1-(1/Sg)]^{1/2}\} \quad (10)$$

Since motion stability depends upon λ being negative, this requirement is met by the following inequality

$$1/Sg \leq S_d(2 - S_d) \quad (11)$$

where

$$1/Sg = I_{yy}\rho d^5 C_{m_\alpha}\pi / 8I^2_{xx}\hat{p}^2 \quad (12a)$$

and

$$S_d = \frac{2[(C^T_{N_\alpha} - C_D) + K_a^{-2}(X_M/2)C^B_{Np_\alpha}]}{C^T_{N_\alpha} - 2C_D - (K_T^{-2}/2)C^{Bc}_{mq}} \quad (12b)$$

The gyroscopic stability parameter $1/Sg$ and the dynamic stability parameter S_d can be used to assess the effect of canards on projectile stability.

There are two conflicting requirements placed upon guided projectile canard design; high projectile maneuverability indicates large canards, while maintenance of projectile stability restricts canard size. A satisfactory design must be a compromise.

A necessary, though not sufficient, condition for projectile stability is that the gyroscopic stability parameter $1/Sg$ not exceed unity. Values of $1/Sg$ between 0.6 and 0.75 are common. Equation (12a) shows that the presence of canards has a detrimental effect on the gyroscopic stability of the round, i.e., increases $1/Sg$. Taking the derivative of the total pitching moment C^T_m in Eq. (1) gives

$$C^T_{m_\alpha} = X_B C^T_{N_\alpha} + X_c C^c_{N_\delta} \quad (13)$$

Since $C^c_{N\delta}$, the canard effectiveness derivative, is based on the reference area S, it may be rewritten based on the area S_c of two canards as

$$C^c_{N\delta} = (S^c/S)\; C_{L_\alpha} \quad (14)$$

to give Eq. (13) as

$$C^T_{M_\alpha} + X_B C^T_{N_\alpha} + (S^c/S) X_c C^c_{L_\alpha} \quad (15)$$

Inserting Eq. (15) into Eq. (12a) gives,

$$1/Sg = I_{yy}\rho d^5 \pi [X_B C^B_{N\alpha} + X_c (S^c/S) C^c_{L_\alpha}] / 8I^2_{xx}\hat{p} \quad (16)$$

Quite clearly, the canard area S^c, and its location X_c, can increase $1/Sg$ over the base-body value. It will subsequently be shown from some wind-tunnel results that, while $C^c_{L_\alpha}(S^c/S)$ is relatively small in comparison with $C^B_{N_\alpha}$ (about 1/6-1/8) the extreme forward position of the canard, i.e., large X_c, causes the canard to have a significant effect on decreasing shell stability.

The effect of the canards on the dynamic stability parameter S_d is less clear. Wind-tunnel testing has indicated that the presence of the canards increases the Magnus moment $X_M C_{N_{p_\alpha}}$, and calculations indicate that canards can increase the pitch damping moment C_{m_q}. Since these quantities appear in a ratio, it would appear that the effect of canards on S_d might be ignored.

Projectile Maneuverability

The third consideration in examining the guided projectile is the effect of canards on weapon maneuverability. The purpose of the canards is to develop a trim angle which, in turn, generates a lift normal to the trajectory. The maneuvering load factor n may be expressed as

$$n = C^T_N QS/W = [C^B_{N_\alpha}\alpha_{ss} - C^c_{N\delta}(\delta - \alpha_{ss})]\; QS/W \quad (17)$$

If Eq. (9) is inserted into Eq. (12) and $C^c_{N\delta}$ is replaced according to Eq. (14), the maneuverability factor n/δ may be written as

$$\frac{n}{\delta} = C^c_{L_\delta}\left[\frac{(X_c - X_B)}{X_B + X_c (C^c_{L\delta}/C^B_{N\alpha})(S^c/S)}\right]\frac{QS^c}{W} \quad (18)$$

It may be seen in Eq. (18) that, as expected, increasing canard area S^c permits an increase in maneuvering load factor n. However, it should also be noted that n is a weak function

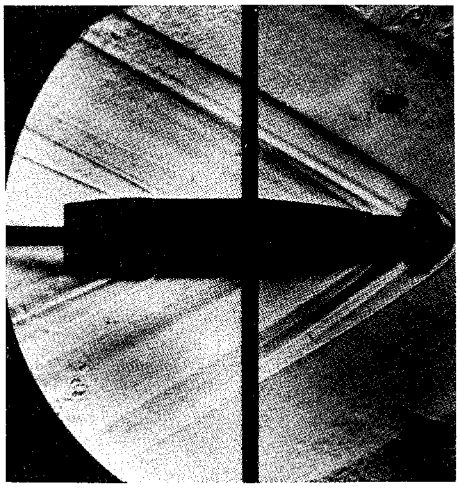

Fig. 6 Schlieren photograph of guided projectile at Mach 2.5.

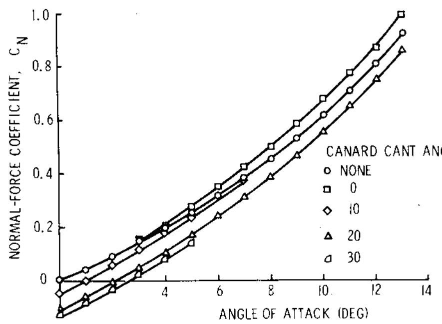

Fig. 7 Normal-force coefficient vs angle of attack at a Mach number of 2.28 and a roll of 0°.

of S^c since S^c appears in both the numerator and in the denominator. An interesting speculation can be made, based on Eq. (18). In the expected operation $(X_c - X_B)$ will always be positive, i.e., canard center of pressure ahead of the body-alone center of pressure. However, the possibility does exist in some applications that, with the forward movement of the body-alone center of pressure with decreasing Mach number, the term $(X_c - X_B)$ changes sign during flight, there would be a control reversal. While control reversal does not occur for the subject guided projectile, the possibility of control reversal must be considered in the design.

Canard Design and Wind-Tunnel Tests

Earlier questions were raised concerning projectile trim, stability, and maneuverability. Relationships from which these three aspects of projectile performance may be considered have been expressed in Eqs. (9,16, and 18). Since the projectile aerodynamic properties expressed in aerodynamic derivatives occur in each of these three equations, it is highly desirable to obtain aerodynamic measurements in a wind tunnel.

The canard configuration selected for testing represented a compromise among stability, performance, and gun-launch enviroment requirements. The location of the canards was more or less fixed by geometrical constraints. The exposed span was limited by the inside diameter of the gun. Within these geometric constraints, the product $X_c C^c_{N_\delta}$ was selected such that the gyroscopic stability criterion would be satisfied.

Several aspect-ratio and planform combinations were examined to select a minimum planform area configuration which satisfied the incremental pitching moment. It was also desirable that the exposed fins be completely within the bow shock over the entire flight regime to preclude nonlinearities in the aerodynamic loads.

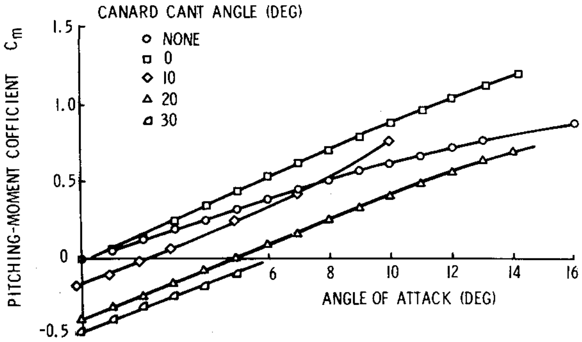

Fig. 8 Pitching-moment coefficient vs angle of attack at a Mach number of 2.28 and a roll angle of 0°.

The launch environment imposes longitudinal accelerations on the order of $10^4 g$ and spin accelerations on the order of 10^6 rad/sec^2 on the canard assembly. Obviously, the fin configuration should attempt to minimize the normal and chordwise bending moments resulting from this environment.

A tapered planform with a taper ratio of 0.4 was selected as the best compromise among the above factors. The airfoil is a 9%, thick double wedge, which was selected from considerations of drag, structural loads, and producibility.

Two sets of wind-tunnel tests were carried out: static measurements to obtain the pitching moment and normal force coefficients, C_m and C_N, and Magnus measurements to obtain the Magnus moment and force derivatives, $C_{n_{p\alpha}}$ and $C_{N_{p\alpha}}$. From the static tests it is possible to obtain the canard effectiveness derivative, $C^c_{N\delta}$, and canard center-of-pressure location X_c; from the Magnus tests $C_{n_{p\alpha}}$ and $C_{N_{p\alpha}}$ are measured directly. The damping-in pitch derivative, C_{m_q}, as required in the equation for the dynamic stability parameter, Eq. (12b), was calculated from the canard effectiveness and center of pressure, $C^c_{N\delta}$ and X_c as

$$C^c_{m_q} = 2X_c^2 C^c_{N\delta} \tag{19}$$

This quantity was added to the contribution of the body-alone $C^B_{m_q}$. For body-alone contributions, available Mk-41 pitch-damping data were used.[2]

Figure 6 shows a two-fifths-scale model of the guided projectile at a Mach number of 2.5 during the static wind-tunnel tests. It will be noted that the canards, at this extreme upper Mach number, are well within the bow shock.

Because of space limitations the wind-tunnel data reduction equations will not be given here. In early tests canard effects, $C^c_{N_\delta}$ and X_c, were obtained by establishing a base line from the projectile without canards. This base line is then subtracted from measurements made on the model with canards in place. In later tests this indirect and less accurate method was replaced by installing a hinge moment balance in a full-scale (though truncated) model to measure the canard load and center of pressure directly. However, even in this second set of tests the entire model was mounted on a five-component balance to provide a check on the hinge moment measurements (by the differential procedure described above), as well as measuring roll torques on the canard frame.

The normal force coefficient vs angle of attack is presented in Fig. 7 for a Mach number of 2.28 and a canard frame roll angle of 0°. A similar presentation of the pitching moment coefficient is given in Fig. 8. In both cases it will be noted that the increase in canard angle, δ, positively (leading-edge downward) results in a downward shift in the curves. The presence of the canard increases the normal force and pitching moment derivatives C_{N_α} and C_{m_α}, as suggested (in the case of the moment) by Eq. (13). Again it is obvious that this effect is greater in the case of the moment than the force derivative. The reason is, of course, that, while $C^c_{N_\delta}$ is only about one-

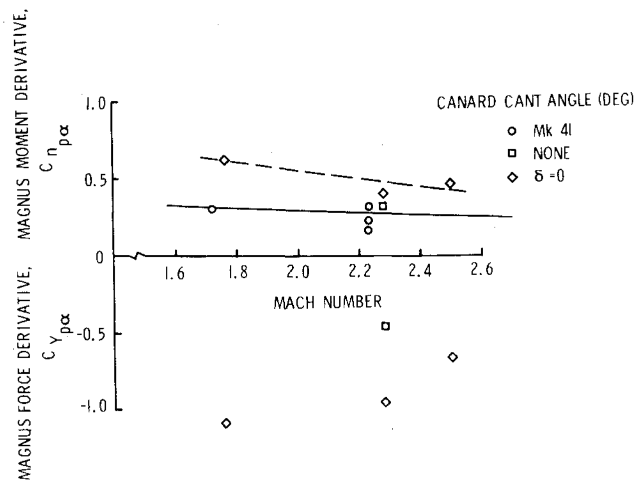

Fig. 9 Magnus force and moment derivatives vs Mach number.

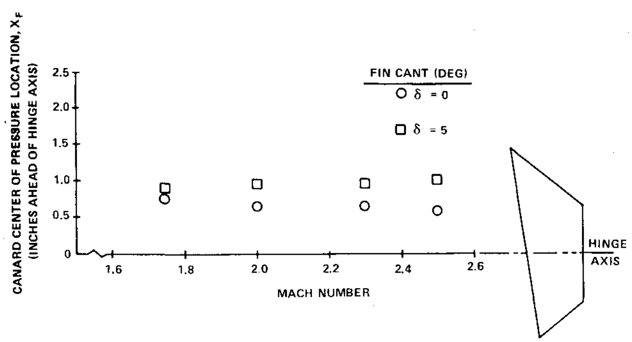

Fig. 10 Canard center of pressure location vs Mach number.

sixth of $C^B_{N_\alpha}$, the forward position of the canard (i.e., large X_c) makes the canard influential in increasing the pitching moment.

Figure 9 indicates some of the Magnus measurements. The Magnus moment is required for determining the dynamic stability parameter [Eq. (12b)]. It will be noted that the Magnus moment and force are increased in the presence of canards.

Finally from the hinge moment measurements it is possible to indicate the center-of-pressure location X_c from the hinge axis of the canard. This result is presented in Fig. 10, where it may be seen (for the 5-in. projectile) that, depending on Mach number and fin deflection, the center of pressure is between ½ and 1 in. ahead of the hinge axis.

Weapon Performance

As a result of these wind-tunnel tests, it is possible to calculate typical values of the gyroscopic and dynamic stability factors, $1/Sg$ and S_d [Eqs. (12b), (16b)] and the projectile maneuverability factor, n/δ[Eq. (18)]. If the following mass and inertial properties are used: $m=1.86$, $K_a^{-2}=7.046$, $K_T^{-2}=0.6099$, and the aerodynamic measurements of which Figs. 7, 8, and 9 are typical, it is possible to obtain at the muzzle and at a Mach number of 2.5

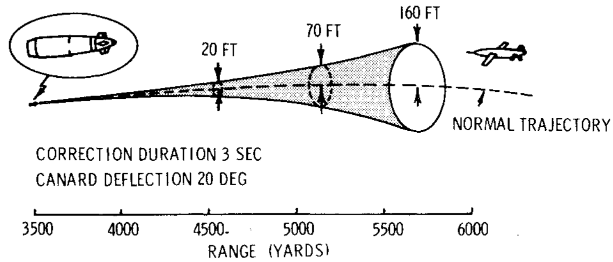

Fig. 11 Guided projectile terminal trajectory.

$$1/Sg=0.860 \quad S_d=0.718 \quad n/\delta=8 \tag{20}$$

If the above value of S_d is inserted into Eq. (11), it will be found that the maximum value of $1/Sg$ for stability is 0.920. Thus, the guided projectile would have marginal gyroscopic stability in the initial part of its flight. Since the reduced spin rate $\hat{p}$ in Eq. (12a) tends to increase downrange, projectile stability will improve downrange.

The maneuverability factor n/δ varies with the square of the Mach number (since the dynamic pressure Q in Eq. (18) varies with Mach number squared for fixed static flow conditions). At the muzzle it may be shown that, for a canard cant angle of 15°, the projectile should be able to acquire a lateral load of about 2 g. As pointed out, this capability will decrease with Mach number squared. Thus, at a Mach number of 1.75 the lateral maneuvering capability will be about 1 g. If it is conservatively assumed that the projectile is capable of 1 g for 3 sec, there will be the capability to maneuver 160 ft, 16,000 ft downrange. This situation is depicted in Fig. 11. Thus the projectile can attain about 10 mils of correction, which was the original design goal.

Conclusion

This preliminary work shows that, from aeroballistic stability considerations a canard-controlled guided projectile is feasible. The weapon should be at least marginally stable over all of its flight. Subsequent unguided firings have substantiated this conclusion. These firings have also shown that there is only about a 2% range degradation with the canards in place. This study has shown that the canards, as designed at present are capable of effecting at leat a 10-mil correction.

References

[1]Murphy, C.H., "Free-Flight Motion of Symmetric Missiles," BRL 1216, July 1963, Ballistic Rearch Labs., Aberdeen Proving Grounds, Md.

[2]Chadwick, W.R., et al., "Dynamic Stability of the 5-in./54 Rocket-Assisted Projectile," NWL TR-2059, Nov. 1966, Naval Surface Weapons Center, Dahlgren Laboratory, Dahlgren, Va.